

Electronic absorption spectra and nonlinear optical properties of CO₂ molecular aggregates: A quantum chemical study[†]

TARUN K MANDAL¹, SUDIPTA DUTTA² and SWAPAN K PATI^{2,3,*}

¹Department of Biotechnology, Haldia Institute of Technology, Haldia 721 657

²Theoretical Sciences Unit and ³New Chemistry Unit,

Jawaharlal Nehru Center for Advanced Scientific Research Jakkur Campus, Bangalore 560 064

e-mail: pati@jncasr.ac.in

Abstract. We have investigated the structural aspects of several carbon dioxide molecular aggregates and their spectroscopic and nonlinear optical properties within the quantum chemical theory framework. We find that, although the single carbon dioxide molecule prefers to be in a linear geometry, the puckering of angles occur in oligomers because of the intermolecular interactions. The resulting dipole moments reflect in the electronic excitation spectra of the molecular assemblies. The observation of significant nonlinear optical properties suggests the potential application of the dense carbon dioxide phases in opto-electronic devices.

Keywords. CO₂; excitonic spectra; nonlinear optical properties.

1. Introduction

The development of materials with large nonlinear optical (NLO) properties has been of great interest in past few decades. These materials find numerous device applications, from lasers to optical switches and electronics.¹ So far, the organic π -conjugated molecules have been considered mostly for this purpose because of their easy functionalization to fine tune the desired properties and the ease of fabrication and integration into devices.^{2–4} In fact, it is the delocalized π -electrons in the organic molecular systems that govern various macroscopic arrangements and thereby show characteristic optical responses. For real applications, these materials can be grown into molecular crystals, either in bulk or in the form of thin films on substrates or as amorphous polymeric systems. In this respect, there exist many other molecular systems, where although there exist π -electrons, they mainly play roles in attaining a particular state of the matter. One such system is carbon dioxide, which exist in various forms of matter, from gaseous to liquid, supercritical liquid and solids. In fact, given the sophistication of experimental advances in recent years, self-assembly of any molecular system can be obtained for desired

electro-optic performances with lower dielectric constants. However, note that, the fabrication of better NLO devices require proper understanding of the geometrical aspects of these molecular aggregates and the forces that stabilize these assemblies.^{5–7}

Earlier we have investigated a few chromophoric aggregates with promising NLO properties.^{5–7} The quest for such structural dependence of NLO properties further motivates us to investigate one of the most well-known and interesting molecule, carbon dioxide (CO₂). The bond dipoles, arising from the partial charge distributions on carbon and oxygen atoms result in significant quadrupole moment. However, the two bond dipoles cancel out each other, leading to a non-dipolar structure because of its linear geometry with $D_{\infty h}$ symmetry. The high polarizability value of CO₂, which is almost comparable with that of HCl, suggests the softness of its electronic cloud, indicating it as a promising candidate for NLO devices in self assembled geometry.⁸ The NLO properties of gaseous CO₂, which is effectively the monomeric response because of the negligible interactions within the neighbouring molecules in gas phase, has been studied earlier.^{9–13} It would thus be of fundamental interest to explore theoretically the dependence of its NLO response functions in dense aggregates. CO₂ molecule in supercritical phase shows unique characteristics of liquid-like density and gas-like diffusivity in addition to its non-

[†]Dedicated to the memory of the late Professor S K Rangarajan

*For correspondence

toxic behaviour, as observed in neutron diffraction experiments.^{14–16} It has been observed in some earlier studies that, due to close proximity of the monomers in these dense phases, the CO₂ molecules no longer remain linear,^{17–20} giving rise to instantaneous dipole moment. Thus we believe, which can be understood in the light of their linear and nonlinear optical response functions. In the present study, we have considered a few possible aggregates of varying special orientations with n ($= 2–4$) CO₂ molecules and studied their geometrical stabilities and NLO responses within the quantum chemical theory framework.

2. Computational method

Geometries of all the molecular aggregates have been relaxed within Möller-Plesset perturbation theory up to second order (MP2), as implemented in Gaussian 03 package.²¹ We consider 6-31++g (*d*) polarized basis set. The dispersion forces play a key role in stabilization of these van der Waal molecular assemblies. MP2 level of calculations are known to capture these forces very well. Having the optimized geometries, we adopt the many body configuration interaction (CI) level of calculation with single excitations to compute the self-consistent field (SCF) molecular orbital energies, the spectroscopic properties and the NLO coefficients using the Zerner INDO (ZINDO) method.²² The single CI is known to reproduce well the experimental spectroscopic and NLO results.²³ Considering the Hartree–Fock (HF) ground state as the reference state, we consider eight occupied and eight unoccupied molecular orbitals for electronic excitations to construct the CI space. To calculate the spectroscopic and NLO properties, we use correction vector method,²⁴ which implicitly assumes all the excitations to be approximated by a correction vector. Given the Hamiltonian matrix, the ground state wave function, and the dipole matrix, all in CI basis, it is straightforward to compute the electronic absorption spectra and the dynamic nonlinear optical coefficients using either the first-order or second-order correction vectors. The details of these methods have been published elsewhere.^{25–27} For consistency check, we also compute the linear and first order nonlinear optical coefficients within the MP2 level of calculation.

3. Structure and geometry

All the optimized molecular aggregates has been shown in figure 1. The optimized geometry of single

CO₂ molecule has symmetrical C–O bond lengths, $d_{C-O} = 1.18075 \text{ \AA}$ with perfectly linear geometry (M). We have arranged several single molecular optimized structures in different special orientations and optimized further the molecular aggregates to obtain the cluster geometry, which can be seen possibly in dense CO₂ phases like supercritical one.^{17–19} The calculated binding energies for these molecular assemblies are given in table 1. As can be seen, the dimer with slipped parallel geometry (D1) is slightly stabler than the T-shape one (D2). The O–C–O angle of both the molecules changes to 179.84° upon optimization in case of the D1. In fact, in the D1 geometry two C–O bonds from two different monomers come closer resulting in electrostatic repulsion between the bond pairs, making the CO₂ molecules effectively nonlinear. However, in case of the T-shape dimer, one of the molecules remains linear, making the O–C–O angle of the other more tilted ($\angle O-C-O = 179.38^\circ$) because of enhanced oxygen lone pair and C–O bond pair repulsions.

All the trimers, except the cyclic planar geometry (T3) show comparable binding energies. The T3 geometry is the most stable structure among the all possible trimers,¹⁸ because of enhanced number of Lewis acid–Lewis base interactions within the CO₂ molecules. The O–C–O angle in this case becomes 179.25° for all the three molecules. It is due to the fact that, the attractive electrostatic forces between carbon and oxygen acts in opposite direction with respect to the repulsive electrostatic forces between the neighbouring oxygen molecules within the hexagonal cyclic geometry. For rest of the trimers, the bond angle distortion is less prominent and asymmetric because of their structural asymmetry compared the T3 geometry. The T4 species resembles the D2 structure and shows similar behaviour.

Among the two quadrumeric structures, the planar Q1 species show lower stability in comparison to tetrahedral Q2 which consists of four CO₂ molecules, sitting at four apex of one tetrahedron. The latter geometry is highly anisotropic with different O–C–O angles for the monomers, resulting from varying distances within them with anisotropic forces.

4. Excitation spectra

The electronic absorption spectra of dipolar aggregates in different spatial geometries can be explained in terms of two state exciton splitting model. It is

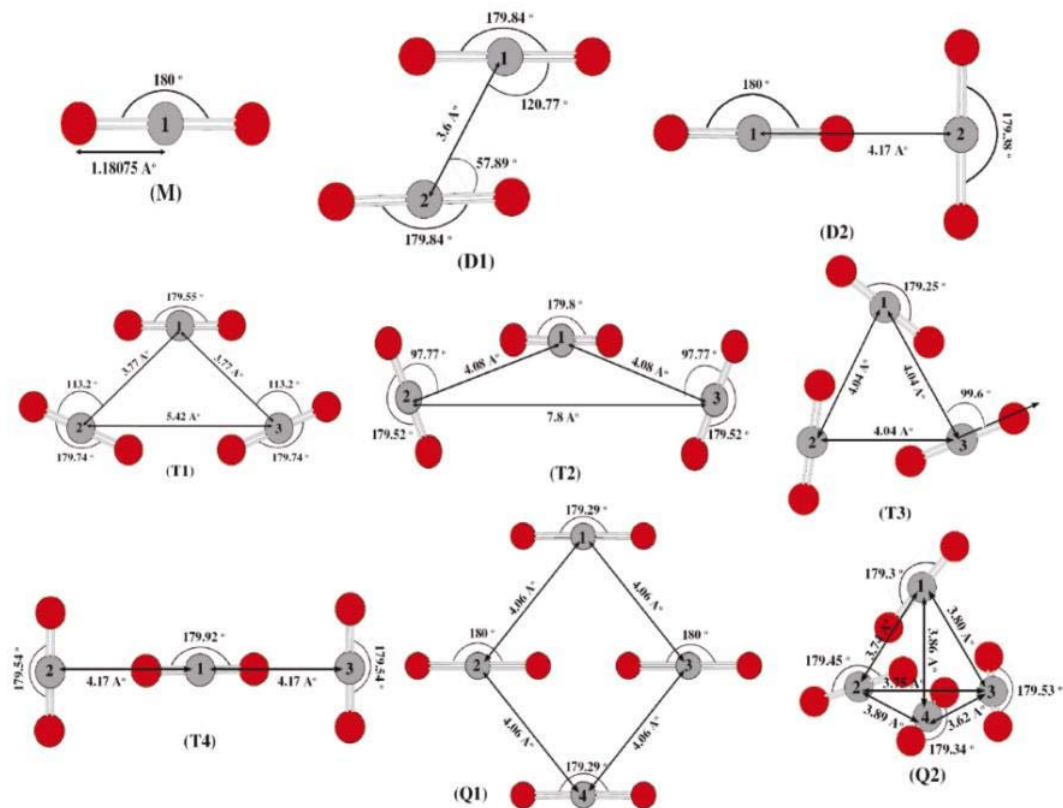


Figure 1. Optimized geometries of molecular aggregates of CO₂: monomer (M), two dimers (D1 and D2), four trimers (T1, T2, T3 and T4) and two quadrupers (Q1 and Q2).

Table 1. Ground state energy (eV), binding energy (eV) and dipole moment (Debye) of all the molecular aggregates considered.

Molecular species	Ground state energy (eV)	Binding energy (eV)	Dipole moment (D)
M	-5119.066		0.00000
D1	-10238.20	-0.0727	0.007615
D2	-10238.20	-0.0680	0.207322
T1	-15357.35	-0.1492	0.098621
T2	-15357.34	-0.1397	0.122581
T3	-15357.41	-0.2121	0.000000
T4	-15357.34	-0.1384	0.000856
Q1	-20476.51	-0.2484	0.000031
Q2	-20476.67	-0.4034	0.068796

well known that, an excitonic state is a result of electron correlations and the excitonic theory is the interaction theory between these excitonic states. The molecular exciton theory can successfully treat the excited state resonance interaction between the molecules in van der Waal aggregates, including molecular crystals, dimers, trimers and of higher orders. In self-assembled aggregates with low packing densities, the excitons are considered to be

Frenkel type excitons where the electron and hole of a mono-excitation are located on the same molecular site.

For dipolar molecules, the lowest optically allowed energy state is an exciton state, and the interactions between these states can be expressed in the direct product basis of the interacting molecular orbitals if the direct overlap between the molecular orbitals is negligible.²⁸⁻³³ This can be realized only at large dis-

tances and thus the coupling between dipolar molecules can be approximated at large distances by a point dipole model. If two molecular species, m and n, are the same, the coupling interactions can be written as,

$$H_{m,n} = \frac{\vec{\mu}_{ij} \cdot \vec{\mu}_{ij}}{r_{mn}^3} - \frac{3(\vec{\mu}_{ij} \cdot \vec{r}_{mn})(\vec{\mu}_{ij} \cdot \vec{r}_{mn})}{r_{mn}^5}, \quad (1)$$

where $\vec{\mu}_{ij}$ is the transition dipole moment from state i to state j of the monomer molecule and \vec{r}_{mn} is the distance between the two molecular centers, m and n, as shown in figure 2. It is to be noted that both the transition dipole ($\vec{\mu}_{ij}$) and the distance (\vec{r}_{mn}) are vectorial quantities. Thus depending on the spatial orientation of the dipoles, the interactions in an aggregate will be governed uniquely by the angle between the two dipoles (ϕ) and the angles that the dipolar axes make with each of the molecular axes (θ), as shown in figure 2. The equation for the dipolar splitting can be directly derived from the above equation as,

$$\Delta E = 2 \frac{\mu_{g,s}^2}{r_{mn}^3} (\cos \phi - 3 \cos^2 \theta), \quad (2)$$

where $\mu_{g,s}$ is the transition dipole from the ground state to the excited state of a single molecule. Therefore, a singlet excited state of the monomer molecule would split according to the angles, (θ and ϕ) and the relative distance among them.

In the present case also, one could expect the excitonic splitting of the monomeric spectra for the interacting molecular aggregates. Although, the single CO_2 molecule is nonpolar, in the aggregates the

deviation in the linearity of CO_2 molecules induces finite dipole moments in each monomer. Moreover, the asymmetric arrangement of the monomers within a cluster results in finite dipole moments for the cluster as a whole, which is shown in table 1. In figure 3, we have shown the electronic absorption spectra of CO_2 molecular aggregates along with the monomer spectra (gas phase spectra), as obtained from many body singles CI calculations. It is clear from the spectral distribution that, the absorption peaks for the gas phase spectra indeed splits in case of the molecular assemblies because of the enhanced intermolecular interactions, suggesting visible spectroscopic response of CO_2 with increasing density. But, the extent of splitting is very small because of less number of interacting neighbours in the systems considered. However, we anticipate very strong spectroscopic response in larger molecular clusters. The significant vibrational spectroscopic response has been observed earlier for some the molecular aggregates considered.^{34–38}

5. Polarizability (α)

As discussed earlier, instead of its nonpolar nature, CO_2 molecule shows very high polarizability value, suggesting the softness of its electronic cloud towards the external perturbations, like electric field or electromagnetic radiation. The polarizability depends linearly on the applied field. The change of frequency dependent polarizability with the strength of electromagnetic radiation is shown in figure 4. The polarizability of monomer shows monotonic increase with the increasing frequency. Although, in the dimer structure the similar trend is observed,

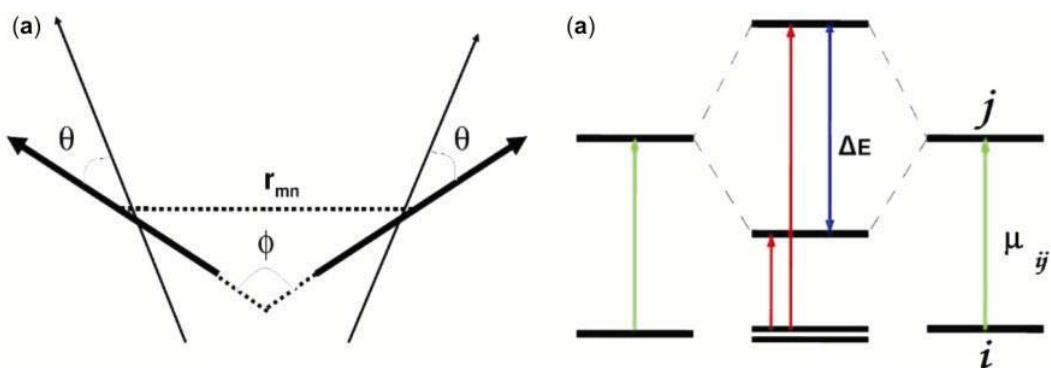


Figure 2. (a) Schematic representation of two interacting dipoles with all the parameters specifying their spatial orientations. (b) Resulting excitonic splitting of the monomeric spectral peak of two interacting monomers.

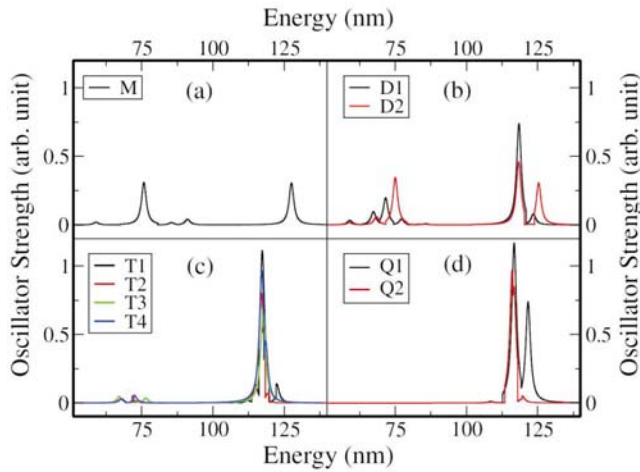


Figure 3. The electronic absorption spectra of (CO₂)_n aggregates with (a) $n = 1$, (b) $n = 2$, (c) $n = 3$ and (d) $n = 4$.

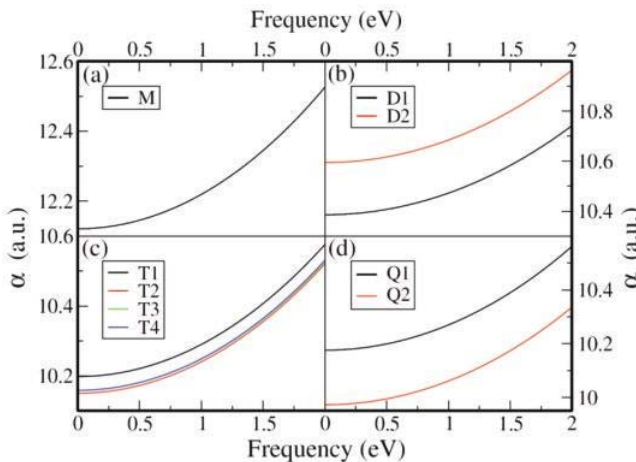


Figure 4. The polarizability per molecule as a function of frequency for the (CO₂)_n aggregates with (a) $n = 1$, (b) $n = 2$, (c) $n = 3$ and (d) $n = 4$.

the rate of change of polarizability with electric field diminishes in comparison to the monomer. However, because of the asymmetric structure, the D2 species shows enhanced polarizability in comparison to the D1 dimer. All the trimers show similar variation in polarizability as a response to the external field. In case of two quadrumeric clusters, the polarizability is higher for the planar geometry (Q1). The reduced polarizability value for the Q2 species can be attributed to the close packed tetrahedral structure which in turn results in stiffness in the electronic cloud. The polarizability values at zero frequency, calculated at MP2 level show close agreement with the CI results, as evident from table 2.

The calculations for spectroscopic and NLO properties are more reliable within the semiempirical ZINDO/CI methodology, because of its better description for the excited states. However, for a comparison, we have presented in table 3 the results obtained from CI singles (CIS) and time-dependent density functional theory (TDDFT) calculations considering the B3LYP exchange correlation function and the 6-31G basis set as implemented in *Gaussian* 03 package²¹ along with ZINDO/CI results. As can be seen, the dipole moment and the polarizability values in all three level of calculations show qualitatively similar trend. However, we would like to point out that, the *ab initio* methods like CIS and TDDFT can not capture the whole range of the excitation spectrum as can be obtained from ZINDO/CI, although the later is semiempirical.

6. Second hyperpolarizability (γ)

The second hyperpolarizability shows monotonic increase with increasing field strength, as shown in figure 5. The behaviours of the molecular aggregates resemble the polarizability variations, except in case of the dimers. Although the dipole moment is significantly higher in D2 arrangement, the D1 species shows enhancement in second hyperpolarizability in comparison to its counterpart. One striking feature can be noticed that, with increase in the number of molecules in the aggregate, the magnitude of the second hyperpolarizability per molecule increases significantly. This behaviour can be directly probed by the enhancement in the density of CO₂ with higher number of molecules in the coordination sphere. Thus, in dense phases like supercritical CO₂ the increased second hyperpolarizability may find potential application in the electro-absorptions and higher order optical responses.

7. First hyperpolarizability (β)

It is well-known that, for non-zero hyperpolarizability which is a first order nonlinear response function, the system should be lacking the center of symmetry.³⁹ In the present study also, we find that, the centrosymmetric structure of the CO₂ monomer gives rise to zero hyperpolarizability. Among all the molecular aggregates considered, only the D2, T2 and Q2 show significant first hyperpolarizability, as can be seen from figure 6. This is due to the fact that the asymmetric spatial orientations of the CO₂ mole-

Table 2. Polarizability and first hyperpolarizability values per molecule for all the molecular aggregates considered, as obtained from MP2 level of calculation for zero frequency.

Molecular species (a.u.)	Polarizability (α) (a.u.)	First hyperpolarizability (β) (a.u.)
M	15.812	0.0102
D1	15.991	0.1901
D2	16.265	1.6580
T1	16.398	0.0991
T2	16.381	0.9048
T3	16.501	0.0820
T4	16.412	0.1544
Q1	16.560	0.0279
Q2	16.470	0.8450

Table 3. The dipole moment (μ), polarizability (α), excitation energy (ΔE) and oscillator strength (f) values of all the molecular aggregates as obtained from configuration interactions singles (CIS), time-dependent density functional theory (TdDFT) and ZINDO level of calculations. Excitation energy and the oscillator strength are given for three lowest excitations. (Note that, the higher energy excitations have non-zero oscillator strengths within ZINDO/CI, as shown in figure 3).

Molecular species	CIS				TdDFT				ZINDO/CI			
	μ (D)	α (a.u.)	ΔE (nm)	f	μ (D)	α (a.u.)	ΔE (nm)	f	μ (D)	α (a.u.)	ΔE (nm)	f
M	0.0	18.11	148.37	0.0	0.0000	14.48	156.13	0.0	0.000	12.12	192.6	0.0
			142.94	0.0			148.86	0.0			185.5	0.0
			142.94	0.0			148.86	0.0			185.5	0.0
D1	0.1425	16.84	147.62	0.0	0.0294	25.93	156.19	0.0	0.008	10.39	191.9	0.0
			147.59	0.0			156.06	0.0			191.9	0.0
			142.30	0.0			149.35	0.0			184.9	0.0
D2	0.3245	15.02	147.97	0.0	0.1623	16.14	156.07	0.0	0.171	10.59	191.8	0.0
			147.58	0.0			155.80	0.0			191.6	0.0
			142.59	0.0			148.85	0.0			184.8	0.0
T1	0.1824	14.02	147.83	0.0	0.0512	28.14	156.39	0.0	0.081	10.20	192.3	0.0
			147.21	0.0			156.26	0.0			192.3	0.0
			142.48	0.0			156.13	0.0			191.3	0.0
T2	0.2013	15.05	147.57	0.0	0.0924	20.32	156.05	0.0	0.112	10.15	191.6	0.0
			147.40	0.0			155.86	0.0			191.6	0.0
			142.18	0.0			155.79	0.0			191.0	0.0
T3	0.0000	16.39	147.03	0.0	0.0006	16.18	155.83	0.0	0.000	10.16	190.7	0.0
			146.96	0.0			155.64	0.0			190.7	0.0
			146.96	0.0			148.67	0.0			190.7	0.0
T4	0.0074	14.35	147.60	0.0	0.0015	19.30	155.95	0.0	0.005	10.15	191.6	0.0
			147.40	0.0			155.81	0.0			191.6	0.0
			142.08	0.0			155.69	0.0			190.9	0.0
Q1	0.0002	14.45	147.74	0.0	0.0005	17.11	156.42	0.0	0.000	10.18	191.8	0.0
			147.72	0.0			156.21	0.0			191.8	0.0
			147.46	0.0			156.02	0.0			191.2	0.0
Q2	0.3124	13.37	147.70	0.0	0.1828	15.88	155.97	0.0	0.090	9.97	190.1	0.0
			146.59	0.0			155.87	0.0			190.0	0.0
			146.46	0.0			155.79	0.0			190.0	0.0

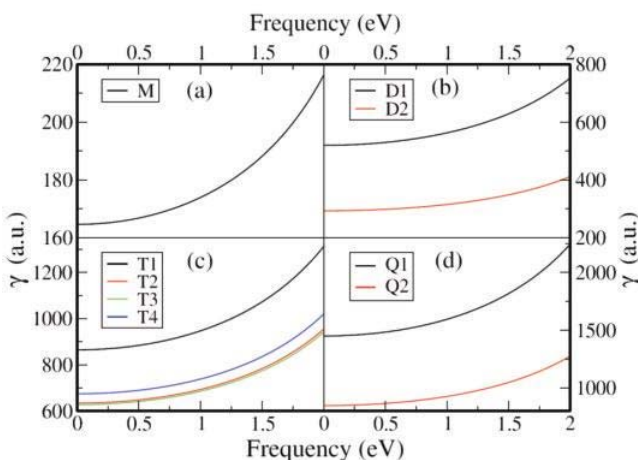


Figure 5. The second hyperpolarizability per molecule as a function of frequency for the (CO₂)_n aggregates with (a) $n = 1$, (b) $n = 2$, (c) $n = 3$ and (d) $n = 4$.

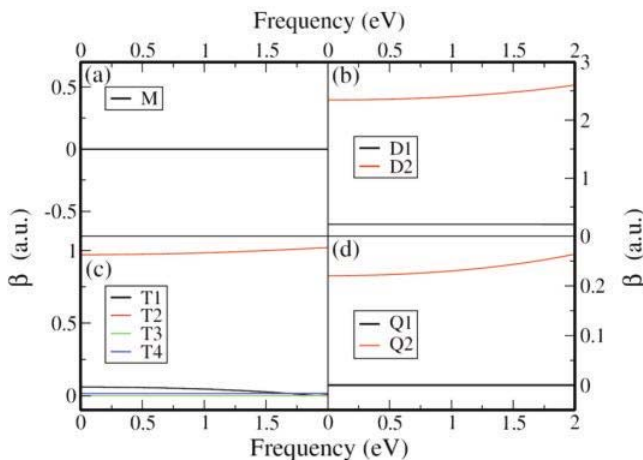


Figure 6. The first hyperpolarizability per molecule as a function of frequency for the (CO₂)_n aggregates with (a) $n = 1$, (b) $n = 2$, (c) $n = 3$ and (d) $n = 4$.

cules in these structures result in non-zero first hyperpolarizability. For rest of the aggregates, the geometrical symmetry suppresses this first order NLO response. These observations are further confirmed from the MP2 level of calculation for zero frequency qualitatively, as can be seen from table 2.

8. Conclusions

We have studied several CO₂ molecular aggregates with dense packing. We find that, the CO₂ molecules no longer remain linear in oligomers due to intermolecular interactions, which results in non-zero dipole moment in each CO₂ molecule. Moreover, depending on the asymmetric spatial arrangement the molecular clusters show instantaneous dipole moment.

Such electronic polarization results in variations in the electronic absorption spectra of these aggregates. Our study clearly shows the close relationship between the structures and the nonlinear responses of the molecular assemblies, which may gain significance in the process of designing efficient opto-electronic devices.

Acknowledgements

TKM acknowledges Jawaharlal Nehru Centre for Advanced Scientific Research (JNCASR) for Visiting Scientist Fellowship. SD acknowledges Council of Scientific and Industrial Research (CSIR), Govt of India for Research Fellowship and SKP acknowledges CSIR and Department of Science and Technology (DST), Govt of India for research funding.

References

- Prasad P N and Williams D J 1991 *Introduction to nonlinear optical effects in molecules and polymers* (New York: Wiley)
- Lindsay G A and Singer K D (eds) 1995 *Polymers for second-order nonlinear optics*, ACS Symposium Series, No. 601 (Washington, DC: ACS)
- Burland D M (ed.) 1994 *Chem. Rev.* **94** 1
- Hanamura E 1988 *Phys. Rev.* **B37** 1273
- Datta A and Pati S K 2006 *Chem. Soc. Rev.* **35** 1305; Datta A and Pati S K 2003 *J. Chem. Phys.* **118** 8420
- Datta A and Pati S K 2004 *J. Phys. Chem. A* **108** 320; Datta A and Pati S K 2004 *J. Phys. Chem. A* **108** 9527; Datta A and Pati S K 2005 *Chem. Eur. J.* **11** 4961
- Datta A, Davis D, Sreekumar K and Pati S K 2005 *J. Phys. Chem. A* **109** 4112; Davis D, Sreekumar K and Pati S K 2005 *Syn. Metals* **155** 384; Datta A and Pati S K 2005 *J. Mol. Struct. (Theochem.)* **756** 97
- Berry R S, Rice S A and Ross J 2000 *Physical chemistry* (Oxford University Press)
- Nir S, Adams S and Rein R 1973 *J. Chem. Phys.* **59** 3341
- Maroulis G and Thakkar A J 1990 *J. Chem. Phys.* **93** 4164
- Maroulis G 1992 *Theor. Chim. Acta* **84** 245
- Sekino H and Bartlett R J 1993 *J. Chem. Phys.* **98** 3022
- Lewis M, Wu Z and Glaser R 2000 *J. Phys. Chem. A* **104** 11355
- Ishii R, Okazaki S, Okada I, Furusaka M, Watanabe N, Misawa M and Fukunaga T 1996 *J. Chem. Phys.* **105** 7011
- Ishii R, Okazaki S, Odawara O, Okada I, Misawa M and Fukunaga T 1995 *Fluid Phase Equilibria* **104** 291
- Ishii R, Okazaki S, Okada I, Furusaka M, Watanabe N, Misawa M and Fukunaga T 1995 *Chem. Phys. Lett.* **240** 84

17. Saharay M and Balasubramanian S 2007 *J. Phys. Chem.* **B111** 387
18. Bhargava B L, Saharay M and Balasubramanian S 2008 *Bull. Mater. Sci.* **31** 327
19. Saharay M and Balasubramanian S 2004 *J. Chem. Phys.* **120** 9694
20. Tsuzuki S, Klopper W and Luthi H P 1999 *J. Chem. Phys.* **111** 3846
21. Gaussian 03, Revision C.02 2004 Frisch M J, Trucks G W, Schlegel H B, Scuseria G E, Robb M A, Cheeseman J R, Montgomery Jr J A, Vreven T, Kudin K N, Burant J C, Millam J M, Iyengar S S, Tomasi J, Barone V, Mennucci B, Cossi M, Scalmani G, Rega N, Petersson G A, Nakatsuji H, Hada M, Ehara M, Toyota K, Fukuda R, Hasegawa J, Ishida M, Nakajima T, Honda Y, Kitao O, Nakai H, Klene M, Li X, Knox J E, Hratchian H P, Cross J B, Bakken V, Adamo C, Jaramillo J, Gomperts R, Stratmann R E, Yazyev O, Austin A J, Cammi R, Pomelli C, Ochterski J W, Ayala P Y, Morokuma K, Voth G A, Salvador P, Dannenberg J J, Zakrzewski V G, Dapprich S, Daniels A D, Strain M C, Farkas O, Malick D K, Rabuck A D, Raghavachari K, Foresman J B, Ortiz J V, Cui Q, Baboul A G, Clifford S, Cioslowski J, Stefanov B B, Liu G, Liashenko A, Piskorz P, Komaromi I, Martin R L, Fox D J, Keith T, Al-Laham M A, Peng C Y, Nanayakkara A, Challacombe M, Gill P M W, Johnson B, Chen W, Wong M W, Gonzalez C and Pople J A Gaussian, Inc., Wallingford CT
22. Ridley J and Zerner M C 1973 *Theor. Chim. Acta* **32** 111; Bacon A C and Zerner M C 1979 *Theor. Chim. Acta* **53** 21
23. Szabo A and Ostlund N S 1996 *Modern quantum chemistry: Introduction to advanced electronic structure theory* (Dover Publications); Dutta S, Lakshmi S and Pati S K 2008 *Phys. Rev.* **B77** 073412
24. Ramasesha S and Soos Z G 1988 *Chem. Phys. Lett.* **153** 171; Soos Z G and Ramasesha S 1989 *J. Chem. Phys.* **90** 1067
25. Ramasesha S, Shuai Z and Bredas J L 1995 *Chem. Phys. Lett.* **245** 224; Albert I D L and Ramasesha S 1990 *J. Phys. Chem.* **94** 6540; Ramasesha S and Albert I D L 1990 *Phys. Rev.* **B42** 8587
26. Pati S K, Ramasesha S, Shuai Z and Bredas J L 1999 *Phys. Rev.* **B59** 14827; Pati S K, Marks T J and Ratner M A 2001 *J. Am. Chem. Soc.* **123** 7287; Pati S K 2004 *Europhys. Lett.* **68** 426
27. Ramasesha S, Pati S K, Krishnamurthy H R, Shuai Z and Bredas J L 1997 *Syn. Metals* **85** 1019; Shuai Z, Bredas J L, Pati S K and Ramasesha S 1997 *Phys. Rev.* **B56** 9298
28. Davydov A S 1962 *Theory of molecular excitons* (New York: McGraw-Hill)
29. Suzuki H 1967 *Electronic absorption spectra: Geometry of organic molecules* (New York: Academic Press)
30. Harada N, Takuma Y and Uda H 1978 *J. Am. Chem. Soc.* **100** 4029
31. Nakanishi K (ed.) 1983 *Circular dichroic spectroscopy: Exciton coupling in organic stereochemistry* (Mill Valley, CA: University Science Books)
32. Scholes G D, Ghiggino K P, Oliver A M and Paddon-Row M N 1993 *J. Am. Chem. Soc.* **115** 4345
33. McCullough J 1987 *Chem. Rev.* **87** 811; Kasha M, 1959 *Rev. Mod. Phys.* **31** 162
34. Jovan Jose K V and Gadre S R 2008 *J. Chem. Phys.* **128** 124310
35. Weida M J, Sperhac J M and Nesbita D J 1995 *J. Chem. Phys.* **103** 7685
36. Weida M J and Nesbita D J 1996 *J. Chem. Phys.* **105** 10210
37. Jucks K W, Huang Z S, Dayton D, Miller R E and Lafferty W J 1987 *J. Chem. Phys.* **86** 4341
38. Fraser G T, Pine A S, Lafferty W J and Miller R E 1987 *J. Chem. Phys.* **87** 1502
39. Datta A 2007 *Theoretical investigations of optical polarizations in chromophoric aggregates and nonlocal charge distributions in clusters* Ph D thesis, JNCASR, Bangalore, www.jncasr.ac.in/pati/ayan_phd.pdf